Eur. Phys. J. D **61**, 579–585 (2011)
DOI: 10.1140/epjd/e2010-10368-7

THE EUROPEAN PHYSICAL JOURNAL D

Regular Article

Electron impact calculations of total elastic cross sections over a wide energy range – 0.01 eV to 2 keV for CH_4, SiH_4 and H_2O

M. Vinodkumar[1,a], C.G. Limbachiya[2], K.N. Joshipura[3], and N.J. Mason[4]

[1] V.P. and R.P.T.P. Science College, 388120 Vallabh Vidyanagar, Gujarat, India
[2] P.S. Science College, 382715 Kadi, Gujarat, India
[3] Department of Physics, S.P. University, 388120 Vallabh Vidyanagar, Gujarat, India
[4] Department of Physics and Astronomy, Open University, Milton Keynes, MK7 6AA, UK

Received 24 June 2010 / Received in final form 19 October 2010
Published online 21 January 2011 –

Abstract. In this paper we report the results of a new theoretical methodology for determining the total elastic electron scattering cross section, Q_{el}, over a wide range of incident energies between 0.01 eV and 2 keV. We have combined results from the UK molecular R-matrix code using Quantemol-N software to determine Q_{el} for incident energies between 0.01 eV and the ionization threshold of the target with calculations based on the spherical complex optical potential formalism for higher energies up to 2 keV. We present results for three selected molecular targets; CH_4, SiH_4 and H_2O as exemplars of the methodology. The present results were found to be in good agreement with previous experimental and theoretical results. The total elastic cross sections for such a wide energy range are reported perhaps for the first time.

1 Introduction

The total electron scattering cross section quantifies the strength of the electron molecule interaction at any particular energy and is an important parameter in many areas of applied science including atmospheric science, astrochemistry, plasma technology and radiation damage. Such total cross sections have been measured by several groups but often such experiments are limited to a fixed energy range and are limited to stable molecular targets easily prepared in the laboratory. Accordingly the development of theoretical methods that are capable of producing reliable, total scattering cross sections for such unstable molecular compounds have been explored for more than two decades with different theoretical methods being developed to treat specific electron interactions (e.g. elastic, excitation and ionization). However these methods are also often limited to specific energy ranges e.g. low energy sub ionization energy methods or high energy regions where semi-classical methods are appropriate and we wish to develop a more general electron scattering methodology that will allow reliable values for total scattering cross sections for electron interaction processes to be calculated over a wide energy region (0.01 eV–2 keV). Combining the results of a low energy scattering code available as a commercial package, Quantemol-N software [1] with a high energy quantum mechanical methodology based on the spherical complex optical potential formalism [2,3]. It should be noted that we do not claim these will be the most accurate or refined cross sections but we wish to present a method that will provide a user of atomic and molecular data with estimated total elastic cross sections (accurate to 5–10%) for input to any model/simulation. This paper presents results of three selected molecular targets; CH_4, SiH_4 and H_2O as exemplars of the methodology that maybe be more widely used to provide data on unstable targets that can not be studied experimentally. Such a methodology may be built into an online electron-molecule/atomic and molecular data base.

Methane, CH_4 is one of the most favored targets in electron-molecule theoretical studies due to its simple structure (nearly spherical), its presence in the atmosphere of the major planets and the observation of several strong features in its total cross sections at very low collision energy, especially the Ramsauer-Townsend minimum and the cross section maximum at about 8 eV. CH_4 has a number of industrial applications including chemical vapor deposition for the production of the artificial diamond and the development of carbon nanotubes and nanocrystalline diamond films [4] process in which electron interactions play a key role.

Silane, SiH_4 plays an important role in plasma-assisted deposition of silicon and amorphous silicon-hydride films. It is also a constituent of the atmosphere of Saturn as well as a minor constituent of the atmospheres of several other planets and their satellites. Formation of SiH_X ($X = 1$–4) radicals by electronic ionization or dissociative ionization of silane is also important for the understanding, the modeling and characterization of the relevant

[a] e-mail: minaxivinod@yahoo.co.in

process chemistry in technological discharge plasmas and also in planetary atmospheres [5].

Water, H_2O is a ubiquitous bio-molecule essential for the existence of life. Any radiation that penetrates the human body produces secondary electrons with appreciable kinetic energies which in turn, subsequently interact with water to liberate free radicals e.g., OH, leading to a variety of biological effects in the human body. Water is also found in most planetary atmospheres playing a key role in their ionospheric chemistry and is abundant in most atmospheric pressure plasmas, often in the form of clusters. Accordingly electron interactions with water are important to the applied science community and are widely studied experimentally, but the polar nature of water complicates both experimental and theoretical studies.

2 Theoretical methodology

The aim of this paper is to show that, by combining two well developed theoretical formalisms, it is possible to provide a self consistent set of data for the total scattering cross section of electrons on polyatomic targets for a wide incident energy range, from 0.01 eV to 2000 eV.

2.1 Low energy formalism; 0.01 eV–15 eV

Ab initio calculations are the most fundamental calculations wherein rigorous mathematical computations are involved. Of the three popular methods for low energy calculations viz. Kohn variational method, Schwinger variational method and the R-matrix method [6], the R-matrix method is used widely [7–9] and the most widely used codes implementing the R-matrix method are the UK molecular R-matrix codes [10], which although freely available, are very difficult for a non-expert to use. Hence we used the Quantemol-N software, which provides a JAVA graphical user interface to the UK polyatomic R-matrix package. This software has been specifically developed as a commercial package capable of being used by non-experts in the applied as well as the basic science community. However we will give details of the underlying principals and methods here.

The basic idea underlying the R-matrix method is the partitioning of configuration space into an inner region and outer region. The boundary of these two regions is selected such that electron charge cloud of the target is negligible at the boundary. In the present case using CH_4, SiH_4 and H_2O as targets we have taken it to be a sphere of radius $10a_o$ centered at the center of mass of the molecule. In the inner region, the scattering electron is indistinguishable from the electrons of the target and the short-range interactions of exchange and correlation forces are dominant. Here methods of quantum chemistry are employed to solve the $N + 1$ eigenvalue problem. When the scattering electron is at a large distance from the center of mass of the target, the probability of such interactions are negligible thereby simplifying the problem in the outer region considerably, and the scattered electron is assumed to propagate in the multipole potential of the target. In the inner region, the wave functions are written as,

$$\psi_k^{N+1} = A \sum \Phi_i^N (x_1, x_2, \ldots, x_N) \sum \xi_j (x_{N+1})\, a_{ijk} + \sum \chi_m (x_1, x_2, \ldots, x_{N+1})\, b_{mk} \quad (1)$$

where A is an antisymmetrization operator, x_N is the spatial and spin coordinate of the Nth electron, Φ_i^N is the ith state of the N-electron target which is represented using a configuration interaction (CI) expansion, ξ_j is a continuum orbital spin coupled with the target states. The coefficients a_{ijk} and b_{mk} are variational parameters which can be determined by solving the $N + 1$ eigenvalue problem in the inner region by employing standard bound state quantum chemistry methods [11]. The standard way of performing a CI target calculation is to use a complete active space CI (CASCI) as this model keeps a balance between the target and scattering calculations [12]. In this model valence electrons are freely distributed amongst the subsets of the valence orbitals.

The occupied and virtual target molecular orbitals are constructed using the Hartree-Fock self-consistent field method using Gaussian-type orbitals (GTOs) and the continuum orbitals used here are those of Faure et al. [13] and include up to g ($l = 4$) orbitals. The advantage of using Gaussian-type orbitals is that infinite integrals are evaluated exactly. In practice, all the integrals are evaluated in the entire configuration space and the tail contribution outside the R-matrix sphere is then subtracted. This can be done efficiently using property integrals for the short-range GTOs. However, treating a large number of coupled states makes the outer region calculations slow since the open-closed portion of the R-matrix at the spherical boundary becomes larger. To overcome this problem most of the strongly closed channels are omitted from the outer region. This technique gives excellent results provided all open states and a few of closed ones are retained in the outer region [14].

Quantemol-N automates the design of a consistent model and simplifies data input requirement. For all the targets we have used C_{2v} symmetry. For methane, we have used the DZP basis set to represent the target molecular orbitals. The electronically excited target states were represented using complete active space (CAS) CI with the carbon $1s$ electrons frozen in all configuration and remaining 8 target electrons freely distributed in the active space between $2a_1$, $3a_1$, $4a_1$, $5a_1$, $1b_1$, $2b_1$, $1b_2$ and $2b_2$ orbitals. In our calculation, Quantemol-N augmented one virtual orbital of each symmetry to continuum orbitals, where orbitals were available to do so. We chose to retain 48 target states, or 300 channels for the construction of the R-matrix at the sphere surface, most of which are strongly closed in the low-energy range considered here. Although the calculation time is much longer, as stated earlier, this results in an improved treatment of polarization interaction, which is crucial in attaining good agreement with available theoretical and experimental data [14]. For silane the target states were represented in the ground state by $1a_1$, $2a_1$, $3a_1$, $1b_1$, $1b_2$, $4a_1$, $5a_1$,

$2b_2$, $2b_1$. We have employed the Hartree-Fock representation where all electrons were frozen in the ground state configuration and hence a static exchange (SE) formalism was employed to describe the scattering wave function. Finally for H_2O, 1s electrons of the oxygen were frozen and remaining 8 target electrons were freely distributed in the active space between $2a_1$, $3a_1$, $4a_1$, $1b_1$, $1b_2$ and $2b_2$ orbitals. For all the cases, in the outer region R-matrix was propagated to $100.1a_0$.

For polar molecules such as H_2O, at the incident energies (<10 eV) the scattering mechanism is largely dominated by the dipole interaction potential, which is non spherical and long range in nature. These dipole interactions give rise to large rotational excitation cross sections at low energies. Therefore for H_2O with a permanent dipole moment of $1.84D$, we have determined the dipole rotational excitation cross sections $Q_{01}(D,\ E_i)$ that is transition for $j = 0$ ground state to $j = 1$ using the first Born approximation.

2.2 Higher energy formalism; 15 eV–2 keV

Since Quantemol-N makes use of R-matrix code, it has the limitation that it can only calculate accurate cross sections below the ionization threshold of the molecule being considered. Beyond the ionization threshold of the target the scattering calculations are carried out using the well established spherical complex optical potential (SCOP) formalism [15–17].

In the SCOP method, the spherical part of the complex optical potential is treated exactly in the partial wave analysis. The complex potential calculation for electron scattering provides total elastic cross sections, Q_{el} and its counterpart total inelastic cross sections, Q_{inel} such that the total scattering cross section (TCS) is given by,

$$Q_T\left(E_i\right) = Q_{el}\left(E_i\right) + Q_{inel}\left(E_i\right). \tag{2}$$

Theoretical studies with strongly polar molecules are difficult as the long range nature of the dipole potential needs the inclusion of large number of partial waves in the scattering calculation. For high partial waves the electrons do not penetrate the wave function of the target molecule. Under these circumstances calculations using the dipole Born approximation are reliable. For a polar molecule such as H_2O, we have determined the dipole rotational excitation cross sections $Q_{01}(D, E_i)$ [16];

$$Q_{TOT}\left(E_i\right) = Q_T\left(E_i\right) + Q_{01}\left(D, E_i\right). \tag{3}$$

The dipole rotational excitation cross sections $Q_{01}(D,\ E_i)$ is calculated using first Born approximation for a molecular dipole of strength D. The explicit general form of the rotational cross section $Q_{01}(D,\ E_i)$ [18] using the point dipole first born approximation for the transition $j = 0$ to $j = 1$ is given by

$$Q_{01}\left(D, E_i\right) BORN,\ PD = \frac{8\pi}{3}\left(\frac{m_e e D}{\hbar^2}\right)\frac{1}{k^2}\ln\left|\frac{k + k_j}{k - k_j}\right|, \tag{4}$$

where $m_e = e = \hbar = 1$ for atomic units and k, k_j are initial and final wave vectors.

Our calculation for these TCSs is based on complex scattering potentials, generated from spherically averaged charge densities of the target. The charge density of lighter hydrogen atoms is expanded at the center of heavier atom (carbon, silicon or oxygen) by employing the Bessel function expansion as in Gradshetyn and Ryzhik [19]. This is a good approximation since it was observed that hydrogen atoms did not significantly act as scattering center and that the cross sections were dominated by central atom size. Thus, the single-center molecular charge density is obtained by a linear combination of constituent atomic charge densities, renormalized to account for covalent molecular bonding.

The molecular charge density is employed to construct a complex optical potential V_{opt}, given by

$$V_{opt}\left(E_i, r\right) = V_R\left(E_i, r\right) + iV_I\left(E_i, r\right). \tag{5}$$

The real part V_R comprises of static potential (V_{st}), exchange (V_{ex}), and polarization (V_p) terms, as follows;

$$V_R\left(E_i, r\right) = V_{st}\left(r\right) + V_{ex}\left(E_i, r\right) + V_P\left(E_i, r\right). \tag{6}$$

We have used the analytical form of the static potential which is derived using the Hartree-Fock wave functions of Bunge et al. [20]. For the exchange potential, we have used parameter free Hara's 'free electron gas exchange model' [21]. And for the polarization potential V_p, we have used parameter free model of correlation polarization potential which contains multipole non-adiabatic corrections in the intermediate region and it smoothly approaches the correct asymptotic form for large 'r' given by Zhang et al. [22]. The imaginary part V_I, also called the absorption potential V_{abs}, accounts for the total loss of scattered flux into all the allowed channels of electronic excitation and ionization. For V_{abs}, we have used the model potential given by Staszewska et al. [23] which is a quasifree, Pauli-blocking, dynamic absorption potential. After generating the full complex potential given in equation (5) for a given electron–molecule system, we solve the Schrödinger equation numerically using partial wave analysis.

At low energies only a few partial waves are significant, e.g. at ionization threshold of the target around 5–6 partial waves are sufficient but as the incident energy increases more partial waves are required. Using these partial waves the complex phase shifts are obtained which are employed to find the relevant cross sections using equation (2). We have neglected the non-spherical terms such as vibrational and rotational potentials in the full expansion of the optical potential. The anisotropic contributions arising from vibrational excitations are very low at the intermediate and high energies. CH_4 and SiH_4 do not possess permanent dipole or quadrupole moments so the rotational cross sections are small and can be neglected in any total elastic cross sections. However we have determined the dipole rotational excitation cross sections $Q_{01}(D,\ E_i)$ using the first Born approximation for H_2O.

3 Results and discussion

The theoretical approach adopted here can be divided into two parts, one using the Quantemol-N formalism up to ionization threshold of the target (∼15 eV) and the other using the SCOP formalism beyond 15 eV. The present results for the three selected molecular targets; CH_4, SiH_4 and H_2O are shown in Figures 1–7 along with available experimental and theoretical comparisons. It is observed that in general there is very good agreement between the present results and all the available data over the entire incident energy range. It should be noted that the results obtained using the two methods (Quantemol and SCOP) match remarkably well at the interface while maintaining the shape and slope of the curve. Moreover, whilst there are minor discrepancies at 15 eV where the two methods overlap, these are well within the experimental error bars and therefore the composite calculation is capable of providing a data set that is self consistent and able to produce a reliable total scattering cross section.

We will now discuss results for each molecule in turn. Figure 1 shows the total elastic cross sections (TECS) for e-CH_4 scattering using both the formalisms discussed in the earlier section of the paper over a wide energy range viz, 0.01 eV to 2000 eV. The transition from the ab initio R-matrix formalism to the SCOP is very smooth as is evident from the figure.

In Figure 2 we have compared the present total elastic cross sections for e-CH_4 scattering with other results reported in the literature. CH_4, has been studied widely over all impact energies considered here. Experimental results are reported by: Boesten and Tanaka (2–100 eV) [24], Bundschu et al. (0.6–5.4 eV) [25], Iga et al. (1–500 eV) [26], Shyn and Cravens (10–50 eV) [27], Sohn et al. (0.2–5 eV) [28], Tanaka et al. (3–20 eV) [29], Vuskovic and Trajmar (20, 30, 200 eV) [30], Sakae et al. (75–700 eV) [31], while theoretical data are reported by Jain (10–2000 eV) [32] and Machado et al. (0.1–50 eV) [33].

The experimental data of Boesten and Tanaka [24] agrees very well with the present results throughout their reported energy range, except at peak where the present results are lower by 5%. Bundschu et al. [25] have reported total elastic cross sections for very low energy (0.6–5 eV) and our results are in excellent agreement beyond 1 eV. Iga et al. [26] have reported elastic cross sections from low to intermediate energy and the present results are in good accord with their data. However our data are slightly higher by 22% than experimental data of Shyn and Cravens [27], this may be due to the extrapolation procedure used by these authors to determine total cross sections from measured differential cross sections and several previous authors have reported similar discrepancies with Shyn and Cravens [27] data in other molecular systems. The measurements of Sohn et al. [28] are for very low energy (0.2 to 5 eV) and present results are in very good agreement beyond 2 eV below which the present values appear to be higher. The measured values of Tanaka et al. [29] compare fairly well at all energies except in the peak region where they are lower by 15% than all other reported values. Vuskovic and Trajmar [30] have measured elastic cross sections for e-CH_4 scattering at 20, 30 and 200 eV. Their experimental values are in very good agreement with ours. The experimental data reported by Sakae et al. [31] are in excellent accord with the present data throughout the range reported by them. The theoretical calculations of Jain [32] are higher by 11% than our present results throughout the energy range. However, the shape of the Jain [32] data curve is similar to the present results. The present results agree well with the theoretical predictions of Machado et al. [33] above 3 eV but

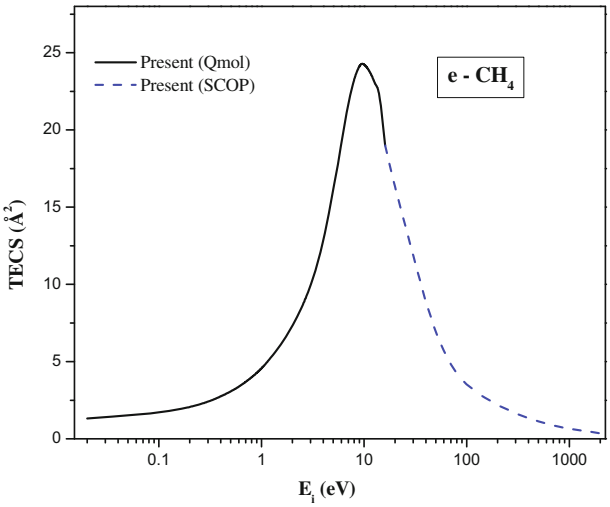

Fig. 1. TECS for e-CH_4 scattering. Solid line (black) → present Q_{el} using Qmol, dash-line (blue) → present Q_T using SCOP.

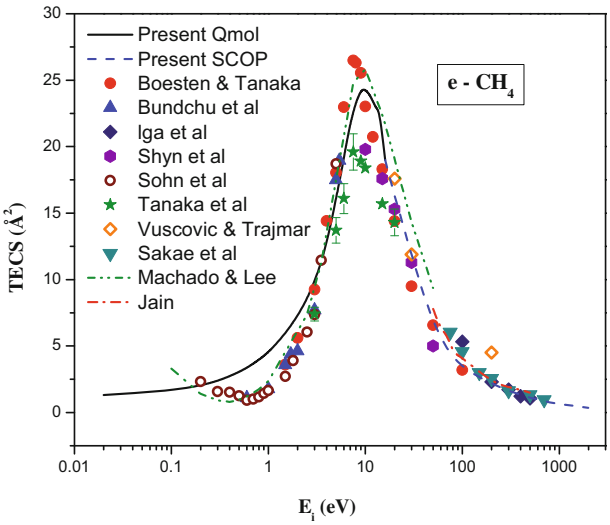

Fig. 2. (Color online) TECS for e-CH_4 scattering. Solid line (black) → present Q_{el} using Qmol, dash line (blue) → present Q_T using SCOP, solid circle → Boesten and Tanaka [24], up triangle → Bundschu et al. [25], diamond → Iga et al. [26], hexagon → Shyn and Cravens [27], open circle → Sohn et al. [28], star → Tanaka et al. [29], open diamond → Vuscovic and Trajmar [30], down triangle → Sakae et al. [31], dash dot → Jain [32], dash dot dot → Machado et al. [33].

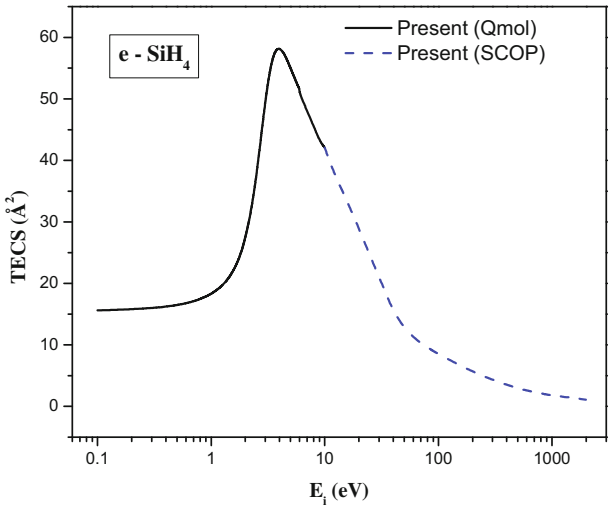

Fig. 3. TECS for e-SiH_4 scattering. Solid line (black) → present Q_{el} using Qmol, dash-line (blue) → present Q_T using SCOP.

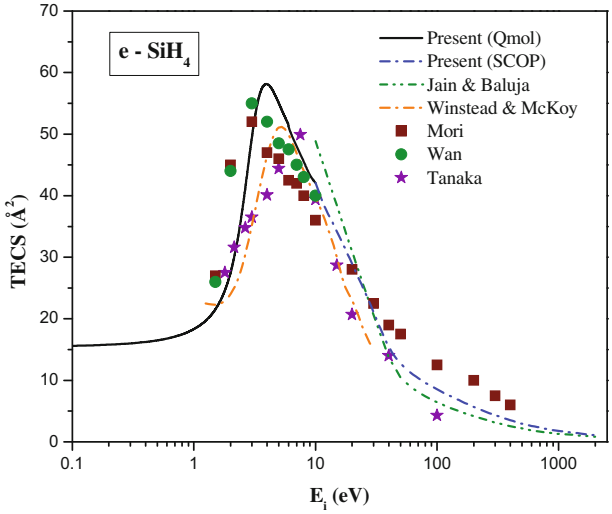

Fig. 4. (Color online) TECS for e-SiH_4 scattering. Solid line (black) → present Q_{el} using Qmol, dash line (blue) → present Q_{el} using SCOP, dash dot dot → Jain and Baluja [39], dash dot → Winstead and McKoy [38], star → Tanaka et al. [34], solid circle → Wan et al. [37], solid square → Mori et al. [35,36].

significant differences of about 60% are observed at lower energies.

In Figure 3 we have shown the total elastic cross sections for e-SiH_4 scattering using R-matrix formalism as well as the SCOP method for the wide energy range 0.01 eV to 2000 eV. The transition from the ab initio R-matrix formalism to the SCOP is also very smooth as noted in the case of methane.

Figure 4 compares the total elastic cross sections for e-SiH_4 scattering with the available data. The experimental results of Tanaka et al. [34] in the range 1.8 eV to 100 eV are in very good agreement with the present results above 10 eV but suggest a peak at higher energies. The measurements of Mori et al. [35,36] show in general good accord

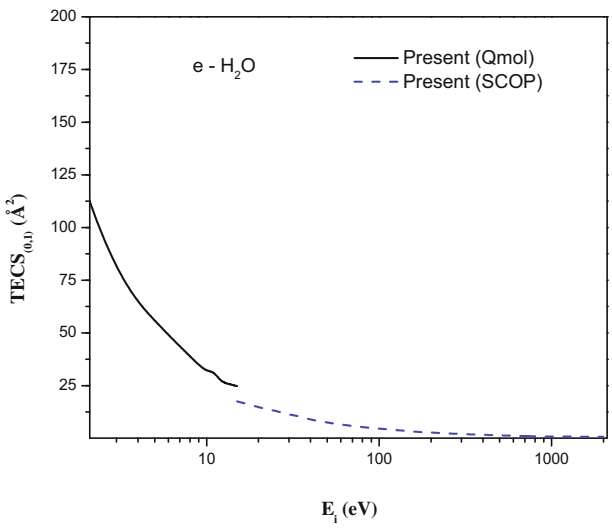

Fig. 5. TECS for e-H_2O scattering. Solid line (black) → present $TECS_{(0,1)}$ using Qmol including rotational cross sections, dash line (blue) → present TECS including rotational cross sections using SCOP.

with present results, with their maximum shifted by 1 eV. Experimental results of Wan et al. [37] are in good agreement with the present results throughout the energy range reported by them. There is also excellent agreement between the theoretical values of Winstead and McKoy [38] throughout the energy range reported by them. Theoretical values of Jain and Baluja [39] are in very good agreement with present data at high energies and they maintain the same shape.

Since H_2O is strongly polar molecule, the contribution of the rotational cross sections is very high at low energies. In Figure 5 we have shown present rotationally summed elastic cross sections for e-H_2O scattering using R-matrix formalism as well as the SCOP method for the wide energy range 0.01 eV to 2000 eV. The transition from the ab initio R-matrix formalism to the SCOP, in this case is not so smooth as non-polar molecules CH_4 and SiH_4. This may be attributed to generally overestimating rotational cross sections at lower energies due to point dipole approximation. It is interesting to note that H_2O has $D = 1.84D$, which is not very small and hence the distortion in lower partial waves particularly at low energy ($E_i < 20$ eV) affects the accuracy of the result [18].

In Figure 6 we have reported present rotationally summed total elastic cross sections from 0.01 eV to 15 eV and compared them with the available results. Recently electron impact studies with benchmark water molecule are carried out theoretically by Zhang et al. [40] at low energies and by Munoz et al. [41] at low to very high energies and experimentally by Khakoo et al. [42]. The rotationally summed elastic cross sections are obtained by adding rotational cross sections to the total elastic cross sections obtained through R-matrix using Qmol program. Present results find good agreement with theoretical results of Zhang et al. [40] at very low energies upto 1 eV, above which the present data are higher by about 40%.

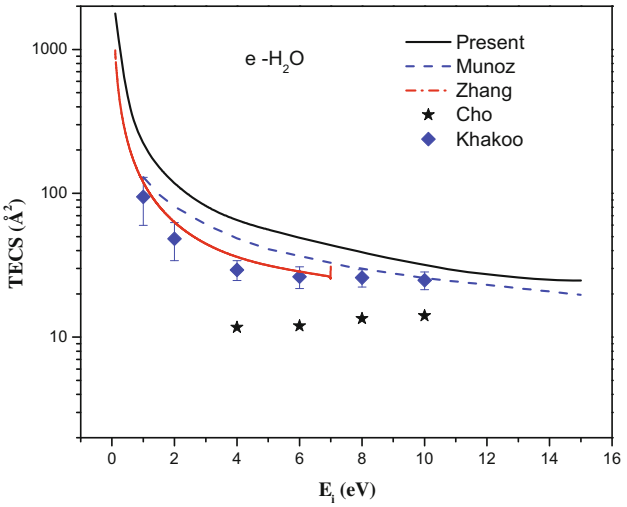

Fig. 6. (Color online) TECS for e-H_2O scattering. Solid line (black) → present TECS using Qmol including rotational cross sections, dash dot line (red) → Zhang et al. [40], dash line (green) → Munoz et al. [41] diamonds → Khakoo et al. [42], star → Cho et al. [43]

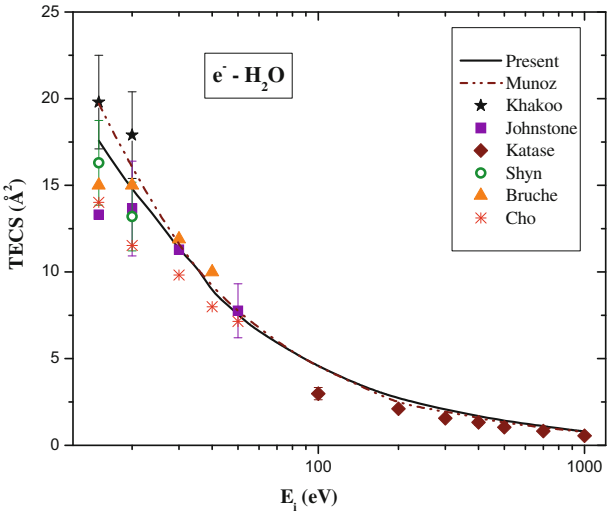

Fig. 7. (Color online) TECS for e-H_2O scattering. Solid line (black) → present TCS using SCOP from 15 eV to 2000 eV, dotted line (red) → Munoz et al. [41], star → Khakoo et al. [42], asterisk → Cho et al. [43], square → Johnstone and Newell [44], open circle → Shyn and Cho [45], diamond → Katase et al. [46], up triangle → Bruche [47,48].

Present results show same nature of the curve with theoretical calculations of Munoz et al. [41] though overestimating by about 25%. While we have used point dipole first Born approximation, Zhang et al. [40] have considered Born top-up procedures in which lower partial waves are obtained using sophisticated treatment [40]. The measurements of Khakoo et al. [42] show same curve shape with the present results but the experimental results of Cho et al. [43] are lower than all the reported data. The data of Cho et al. [43] are integrated cross sections which are lower than measured TCS and may reflect the difficulty of integrating the dipole induced forward peak in the DCS [42]. The estimated error in the derived elastic integral cross sections is less than 23% [43]. We have employed the first Born approximation [18] to calculate rotational excitation cross sections which over estimate all other data due to point dipole approximation.

In Figure 7 we have compared present total rotationally summed elastic cross sections for e-H_2O scattering with available data. H_2O has been investigated extensively by many experimentalists at different energy ranges. The recent theoretical calculations over a wide energy range are due to Munoz et al. (1–1000 eV) [41]. The measurements are due to Khakoo et al. (1–100 eV) [42], Johnstone and Newell (6–50 eV) [44], Shyn and Cho (2.2–20 eV) [45], Katase et al. (100–1000) [46] and Bruche (3–40 eV) [47,48]. The experimental values of Shyn and Cho [45], Johnstone and Newell [44] and Bruche [47,48] are derived from integrated differential cross sections. The experimental results of Katase et al. [46], Johnstone and Newell [44] and Bruche [47,48] are in very good accord with present results. The experimental values of Shyn and Cho [45] are lower compared to all results as discussed by Khakoo et al. [42]. Whereas present results are lower than the theoretical values of Munoz et al. [41] by 33% at 15 eV, they are in excellent agreement beyond 20 eV.

4 Conclusion

In this paper we wish to indicate how, through the combination of two different electron molecule scattering codes (the R-matrix through Quantemol-N for low energies and SCOP for higher energies), it is possible to provide a set of reliable cross sections across a wide energy range (0.01–2000 eV). We have illustrated this methodology for three simple polyatomic molecular targets CH_4, SiH_4 and H_2O for which there exists a good database against which we can benchmark our results. The results are promising with good matching at the transition energy (15 eV) between the two methodologies and good agreement with available data throughout the energy range. Therefore we may have confidence that the methodology may be used to calculate such cross sections in other molecular systems, and particularly may be used to estimate cross sections for electron scattering from molecular targets that can not be easily studied experimentally (e.g. free radicals CF_X and SiH_X or OH).

Such data is needed in a variety of applications from aeronomy to plasma modeling for technology. Accordingly such a methodology maybe built into the design of on-line databases to provide a 'data user' with the opportunity to request their own set of cross sections for use in their own research. Such a prospect will be explored by the emerging virtual atomic and molecular data centre (VAMDC) http://batz.lpma.jussieu.fr/www_VAMDC/.

MVK and CGL thank University Grants Commission New Delhi, for Major Research project under which part of this work is done. MVK and CGL would like to thank Hemal N. Varambhia, UCL, London for fruitful discussion on Quantemol-N software. MVK thanks DST, New Delhi for major research

project. KNJ thanks Indian Space Research Organization – Bangalore for a research Project grant.

References

1. J. Tennyson, D.B. Brown, J.M. Munro, I. Rozum, H.N. Varambhia, N. Vinci, J. Phys. Conf. Ser. **86**, 012001 (2007)
2. M. Vinodkumar, C. Limbachiya, K. Korot, K.N. Joshipura, N. Mason, Int. J. Mass Spectrom. **273**, 145 (2008)
3. M. Vinodkumar, K. Korot, C. Limbachiya, B. Antony, J. Phys. B At. Mol. Opt. Phys. **41**, 245202 (2008)
4. C. Makochekanwa, K. Oguri, R. Suzuki, T. Ishihara, M. Hoshino, M. Kimura, H. Tanaka, Phys. Rev. A **74**, 042704 (2006)
5. M. Vinodkumar, C. Limbachiya, K. Korot, K.N. Joshipura, Eur. Phys. J. D **48**, 333 (2008)
6. P.G. Burke, K.A. Berrington, *Atomic and Molecular Processes, an R-matrix Approach* (Institute of Physics Publishing, Bristol, 1993)
7. P. Kolorenc, V. Brems, J. Horacek, Phys. Rev. A **72**, 012708 (2005)
8. M. Hiyama, N. Kosugi, J. Theor. Comput. Chem. **4**, 35 (2005)
9. S. Tonzani, Comput. Phys. Commun. **178**, 146 (2007)
10. L.A. Morgan, J. Tennyson, C.J. Gillan, Comput. Phys. Commun. **114**, 120 (1998)
11. H. Varambhia, J. Tennyson, J. Phys. B At. Mol. Opt. Phys. **40**, 1211 (2007)
12. J. Tennyson, J. Phys. B At. Mol. Opt. Phys. **29**, 6185 (1996)
13. A. Faure, J.D. Gorfinkiel, L.A. Morgan, J. Tennyson, Comput. Phys. Commun. **144**, 224 (2002)
14. H.N. Varambhia, J.J. Munro, J. Tennyson, Int. J. Mass Spectrom. **271**, 1 (2008)
15. M. Vinodkumar, C. Limbachiya, B. Antony, K.N. Joshipura, J. Phys. B At. Mol. Opt. Phys. **40**, 3259 (2007)
16. M. Vinodkumar, K.N. Joshipura, C. Limbachiya, N. Mason, Phys. Rev. A **74**, 022721 (2006)
17. K.N. Joshipura, M. Vinodkumar, C.G. Limbachiya, B.K. Antony, Phys. Rev. A **69**, 022705 (2004)
18. Y. Itikawa, Phys. Rep. **46**, 117 (1978)
19. I. Gradashteyn, I.M. Ryzhik, *Tables of Integrals, Series and Products* (Associated Press, New York, 1980)
20. C.F. Bunge, J.A. Barrientos, A.V. Bunge, At. Data Nucl. Data Tables **53**, 113 (1993)
21. S. Hara, J. Phys. Soc. Jpn **22**, 710 (1967)
22. X. Zhang, J. Sun, Y. Liu, J. Phys. B At. Mol. Opt. Phys. **25**, 1893 (1992)
23. G. Staszewska, D.M. Schwenke, D.G. Truhlar, Chem. Phys. **81**, 3078 (1984)
24. L. Boesten, H. Tanaka, J. Phys. B At. Mol. Opt. Phys. **24**, 821 (1991)
25. C.T. Bundschu, J.C. Gibson, R.J. Gulley, M.J. Brunger, S.J. Buckman, N. Sannak, F.A. Gianturco, J. Phys. B At. Mol. Opt. Phys. **30**, 2239 (1997)
26. I. Iga, M.T. Lee, G.P. Homem, L.E. Machado, L.M. Brescansin, Phys. Rev. A **61** 022708 (2000)
27. T.W. Shyn, T.E. Cravens, J. Phys. B At. Mol. Opt. Phys. **23**, 293 (1990)
28. W. Sohn, K.H. Kochem, K.M. Scheuerlein, K. Jung, H. Ehrhardt, J. Phys. B **19**, 3625 (1986)
29. H. Tanaka, T. Okada, L. Boesten, T. Suzuki, T. Yamamoto, M. Kubo, J. Phys. B **15**, 3305 (1982)
30. L. Vuskovic, S. Trajmar, J. Chem. Phys. **78**, 4947 (1983)
31. T. Sakae, S. Sumiyoshi, E. Murakami, Y. Matsumoto, K. Ishibashi, A. Katase, J. Phys. B At. Mol. Opt. Phys. **22**, 1385 (1989)
32. A. Jain, Phys. Rev. A **34**, 3707 (1986)
33. L.E. Machado, M.-T. Lee, L.M. Brescansin, Braz. J. Phys. **28**, 111 (1998)
34. H. Tanaka, L. Boesten, H. Sato, M. Kimura, M.A. Dillon, D. Spence, J. Phys. B At. Mol. Opt. Phys. **23**, 577 (1990)
35. S. Mori, Y. Katayama, O. Sueoka, At. Coll. Res. Jpn **11**, 19 (1985)
36. O. Sueoka, private communication
37. H.-X. Wan, J.H. Moore, J.A. Tossell, J. Chem. Phys. **91**, 7340 (1989)
38. C. Winstead, V. McKoy, Phys. Rev. A **42**, 5357 (1990)
39. A. Jain, K.L. Baluja, Phys. Rev. A **45**, 202 (1992)
40. R. Zhang, A. Faure, J. Tennyson, Phys. Scr. **80**, 015301 (2009)
41. A. Munoz, J.C. Oller, F. Blanco, J.D. Gorfinkiel, P. Limao-Vieira, G. Garcia, Phys. Rev. A **76**, 052707 (2007)
42. M.A. Khakoo, H. Silva, J. Muse, M.C.A. Lopes, C. Winstead, V. McKoy, Phys. Rev. A **78**, 052710 (2008)
43. H. Cho, Y.S. Park, H. Tanaka, S.J. Buckman, J. Phys. B At. Mol. Opt. Phys. **37**, 625 (2004)
44. W.M. Johnstone, W.R. Newell, J. Phys. B At. Mol. Opt. Phys. **24**, 3633 (1991)
45. T.W. Shyn, S.Y. Cho, Phys. Rev. A **36**, 5138
46. A. Katase, K. Ishibashi, Y. Matsumoto, T. Sakae, S. Maezono, E. Murakami, K. Watanabe, H. Maki, J. Phys. B **19**, 2715 (1986)
47. E. Bruche, Ann. Phys. Leipzig **83**, 1065 (1927)
48. E. Bruche, Ann. Phys. **1**, 93 (1929)